Copper pathology in vulnerable brain regions in Parkinson's disease.

Katherine Davies, Sylvain Bohic, Asunción Carmona, Richard Ortega, Veronica Cottam, Dominic Hare, John Finberg, Stefanie Reyes, Glenda Halliday, Julian Mercer, et al.

Author manuscript, published in "Neurobiol Aging 2014;35(4):858-66"
DOI : 10.1016/j.neurobiolaging.2013.09.034

Research Article

Copper pathology in vulnerable brain regions in Parkinson's disease

Katherine M. Davies,[1,2*] Sylvain Bohic, PhD,[3,4,5,*] Asunción Carmona, PhD,[6,7] Richard Ortega, PhD,[6,7] Veronica Cottam,[1] Dominic J. Hare, PhD,[8,9] John P.M. Finberg, PhD,[10] Stefanie Reyes,[1,2] Glenda M. Halliday, PhD,[1,2] Julian F.B. Mercer, PhD,[11] Kay L. Double, PhD,[1,2,12]

1- Neuroscience Research Australia, Sydney, NSW, Australia

2- School of Medical Sciences, Faculty of Medicine, University of New South Wales, Sydney, Australia

3- Inserm, U836, team 6, Rayonnement Synchrotron et Recherche Médicales, Grenoble Institut des Neurosciences, Grenoble, F-38042, France

4- European Synchrotron Radiation Facility, ESRF, BP220, Grenoble, F-38043, France

5- Université Joseph Fourier 1, Grenoble Institut des Neurosciences, Grenoble, France

6- University of Bordeaux, CENBG, UMR 5797, F-33170 Gradignan, France

7- CNRS, IN2P3, CENBG, UMR 5797, F-33170 Gradignan, France

8- Elemental Bio-imaging Facility, University of Technology Sydney, Australia

9- The Florey Institute of Neuroscience and Mental Health, University of Melbourne, Parkville, Australia

10- Faculty of Medicine, Technion, Haifa, Israel

11- Centre for Cellular and Molecular Biology, Deakin University, Melbourne, Australia

12- Discipline of Biomedical Sciences, School of Medical Sciences, Sydney Medical School, The University of Sydney, NSW Australia

* joint first authors

Correspondence to:

Kay L. DOUBLE
Discipline of Biomedical Sciences
School of Medical Sciences
Sydney Medical School
The University of Sydney
Cumberland Campus C42
75 East St (PO Box 170)
Lidcombe NSW 2141
Australia
Email: kay.double@sydney.edu.au
Tel: (+) 61 – 2 9351 9357

Sylvain BOHIC
Inserm U-836
Grenoble Institute of Neuroscience
Team 6: Rayonnement Synchrotron
C42 et Recherches Médicales
ESRF
Rue Jules Horowitz
BP220
F-38043 Grenoble Cedex
Email: bohic@esrf.fr
Tel : (+) 33 – 476 – 882 – 852

Running heading: Copper pathology in PD

Number of characters in the title: 67 (with spaces)

Number of characters in the running head: 22 (with spaces)

Number of words in the abstract: 152

Number of words in the body of the manuscript: 4304

Number of figures: 7 of which 3 are in color (2 supplementary figures)

Number of tables: 0 (6 supplementary tables)

Number of references: 45

Abstract

Synchrotron-based X-ray fluorescence microscopy, immunofluorescence, and western blotting were used to investigate changes in copper (Cu) and Cu-associated pathways in the vulnerable substantia nigra (SN) and locus coeruleus (LC), and non-degenerating brain regions, in cases of Parkinson's disease (PD) and appropriate healthy and disease controls. In PD and incidental Lewy body disease (ILBD), levels of Cu and Cu transporter protein 1 (Ctr1), were significantly reduced in surviving neurons in the SN and LC. Specific activity of the cuproprotein superoxide dismutase 1 (SOD1) was unchanged in the SN in PD but was enhanced in the parkinsonian anterior cingulate cortex (ACC), a region with α-synuclein pathology, normal Cu and limited cell loss. These data suggest that regions affected by α-synuclein pathology may display enhanced vulnerability and cell loss if Cu-dependent protective mechanisms are compromised. Further investigation of copper pathology in PD may identify novel targets for the development of protective therapies for this disorder.

Keywords: copper; copper transporter 1 (Ctr1); human brain; Parkinson's disease; substantia nigra; superoxide dismutase 1 (SOD1)

1. Introduction

Neurodegenerative cascades in Parkinson's disease (PD) involve protein aggregation and oxidative stress, although the triggers for these events are unknown. Changes in biometals have long been suspected to play a role in these cascades. Copper (Cu) is an important biometal in the brain, as exemplified by Menkes and Wilson's diseases; serious neurological disorders of Cu dyshomeostasis (de Bie et al., 2007; Schaefer and Gitlin, 1999). A significant decrease in total tissue Cu in the degenerating substantia nigra (SN) in PD has been consistently reported over a number of decades (Ayton et al., 2012; Dexter et al., 1989; Loeffler et al., 1996; Popescu et al., 2009; Uitti et al., 1989) and recent evidence suggests that peripheral Cu metabolism is altered in PD (Larner et al., 2013). The complexing of Cu with the PD-associated protein α-synuclein increases aggregation and toxicity of this protein (Rose et al., 2011; Wang et al., 2010), possibly via stimulation of free radical production (Meloni and Vasak, 2011). On the other hand, Cu is also a critical cofactor in a range of cuproproteins, including the key protective cellular antioxidant superoxide dismutase 1 (SOD1) (McCord and Fridovich, 1969). Studies in model systems demonstrate that Cu depletion is associated with reduced activity of SOD1 and a concomitant increase in free radical production, which can be normalized by Cu supplementation (Lombardo et al., 2003; Prohaska, 1983). SOD1 activity is reduced in the plasma of PD patients (Torsdottir et al., 2006) and studies in animal models of PD suggest that overexpression of SOD1 increases neuronal survival (Battaglia et al., 2002; Botella et al., 2008; Tripanichkul et al., 2007). These data suggest that a reduction in brain Cu in PD may reduce SOD1-mediated antioxidant defense and contribute to neurodegenerative cascades. In the following work, we investigated changes in neuronal Cu levels and transport pathways to determine if changes in Cu are associated with a reduced antioxidant capacity in regions of neurodegeneration in PD.

2. Methods

2.1. Brain tissue samples

Brain tissue samples were requested and received from the New South Wales Tissue Resource Centre at the University of Sydney and the Sydney Brain Bank at Neuroscience Research Australia. The brain tissue samples were from patients with idiopathic PD and incidental Lewy body disease (ILBD), identified according to the diagnostic criteria of Dickson et al. (Dickson et al., 2009), and from Alzheimer's disease (AD) and age-matched controls, identified according to the diagnostic criteria of Montine et al. (Montine et al., 2012) (Supplementary Tables 1, 2 and 3). All cases of PD had received anti-parkinsonian medications prior to death, but none of the ILBD, AD, or control cases had received dopamine-replacement therapies. Cases with other neurological or neuropathological conditions were excluded and consent to use autopsy material for research purposes was obtained for all cases.

Brain regions investigated included the SN and locus coeruleus (LC), the brain regions most vulnerable to neuronal loss and Lewy body pathology in PD, the anterior cingulate cortex (ACC) which is affected by Lewy body pathology later in the course of PD and has limited cell loss, and the occipital cortex (OCx), a non-degenerating region in PD (Braak et al., 2003; Harding et al., 2002). Samples were collected within 48 hours of death, dissected using polytetrafluoroethylene-coated blades (ProSciTech, Queensland, Australia), and the fresh tissue samples frozen immediately in liquid nitrogen, then stored at -80°C prior to analysis. Fixed tissue samples were stored in formalin prior to cryo-microtome sectioning. Due to limited tissue availability, not every brain region was used in every experiment.

2.2. Measurement of neuronal and regional Cu levels

Total Cu levels within cells are the sum of different pools of Cu; free Cu and Cu bound to proteins. In the brain the majority of Cu is not free but is tightly regulated by being bound to a range of molecules, including Cu transport proteins and other molecules, such as neuromelanin (Bohic et al., 2008), an intracellular pigment found in vulnerable regions of the PD brain (Hirsch et al., 1988). Total Cu levels were quantified within single neurons as well as regions in thin sections (20 μm) cut from fixed or frozen tissue samples using synchrotron radiation X-ray fluorescence microscopy (SRXFM) and particle induced X-ray emission (PIXE) microscopy. Experiments were conducted using the microprobes endstation at ID22 beamline of the European Synchrotron Radiation Facility and at the Diamond Light Source I18 beamline, as previously described (Antharam et al., 2012; Bohic et al., 2008). Micro-PIXE and micro-backscattering spectrometry (BS) analyses were performed simultaneously using the AIFIRA (Applications Interdisciplinaires des Faisceaux d'Ions en Région Aquitaine) facility to enable quantitative chemical analysis of trace elements in cells and tissues (Carmona et al., 2008). For each case (Supplementary Table 1) two fixed tissue sections of the SN, LC and OCx were investigated: one using SRXFM to raster-scanned individual pigmented neurons (6-10 per section/case) with a step size of 1 μm; and the other using PIXE microprobes to raster-scan over a 683 μm x 683 μm area, corresponding to the larger scan size available for incident protons of 3.0 MeV energy. In the SN and LC, only neurons exhibiting normal pigmented morphology were chosen to avoid measurement of extraneuronal neuromelanin (NM) pigment. Elemental concentrations derived from single neurons analyzed in each section were averaged and only one value from each patient was used in the analysis. Results from fixed tissue were confirmed in the SN using the same methods on fresh frozen tissue sections from PD and control cases (Supplementary Table 2).

For quantification of whole tissue Cu content, samples of fresh frozen brain (35-60 mg)

from the SN, ACC and OCx were subjected to closed-vessel microwave digestion (Milestone MLS1200) in 4 mL of concentrated nitric acid and 1 mL 35% hydrogen peroxide (both Seastar Chemicals, British Columbia, Canada). Digests were diluted w/w to c.a. 50 g with 1% nitric acid, and total metal concentrations were determined using an Agilent Technologies 7500cs inductively coupled plasma mass spectrometer (ICP-MS) (Forrest Hill, Victoria, Australia), as previously described (Davies et al., 2013). Specificity for Cu was confirmed by measuring both m/z 63 and 65. Cu levels in the SN (subsequently referred to as TH-associated Cu levels) were calculated relative to nigral tyrosine hydroxylase determined by Western blot, as an index of dopamine neuron loss.

2.3. Preparation of brain tissue proteins for Western blotting and activity assays

Samples from fresh frozen brain (62-84 mg) from the SN, ACC and OCx were homogenized in 17 volumes of buffer solution (10 mM Tris-HCl, 0.25 M sucrose and 1 mM EDTA, pH 7.4) using a hand-held electric homogenizer with a polycarbonate probe (OmniTH, Kelly Scientific, Australia). For assaying SOD activity, homogenates of brain tissue proteins were centrifuged at 1,500 g for 5 min at 4 °C. For Western blot analysis, 1% SDS and 1:50 dilution of protease inhibitor cocktail (Sigma) was added to homogenates of brain tissue proteins before being centrifuged at 10,000 g for 15 min at 4 °C. Supernatants were collected and stored at -80 °C. Pierce® BCA Protein Assay Kit (Thermo Scientific) was used to determine sample protein concentration.

2.4. Primary antibodies used for detection of Cu transport proteins using Western blotting and immunohistochemistry

Primary antibodies used are detailed in Supplementary Table 4. Specificity of each antibody was confirmed by including no primary antibodies and, for Atox1, by preadsorption of the Atox1 antibody with the antigen against which the primary antibody was raised (the antigen

was not available for the other antibodies used). The ATPase antibodies used in this study have been well characterized in previous reports, and their specificity confirmed (Cater et al., 2007; Ke et al., 2006). Horseradish peroxidase-conjugated antibodies used for detection of proteins by Western blotting include: mouse anti-goat IgG, goat anti-mouse IgG, and donkey anti-sheep/goat IgG (all Millipore, USA). Fluorescent antibodies used for detection of proteins include: donkey anti-goat Alexa Fluor® 594 IgG (H+L), donkey anti-sheep Alexa Fluor® 594 IgG (H+L), donkey anti-sheep Alexa Fluor® 488 IgG (H+L), donkey anti-mouse Alexa Fluor® 594 IgG (H+L), and donkey anti-rabbit Alexa Fluor® 488 IgG (H+L), all purchased from Invitrogen (Eugene, Oregon, USA).

2.5. SDS-PAGE and Western blot analysis of Cu transport proteins

The following protein amounts were loaded onto 4-12% Bis-Tris Criterion pre-cast gels (Bio-Rad); Copper transporter 1 (Ctr1): 40 μg, Atox1: 80 μg, ATP7A: 100 μg, ATP7B: 100 μg, SOD1: 2.5 μg, Tyrosine Hydroxylase (TH): 40 μg, and separated by SDS-PAGE in MES (Atox1) or MOPS (Ctr1, ATP7A, ATP7B, SOD1, TH) buffer (Bio-Rad), according to manufacturer's instructions (Bio-Rad). Separated proteins were transferred to Immobilon- P^{SQ} PVDF (Millipore) (Ctr1, Atox1, SOD1, and TH) or nitrocellulose (Millipore) (ATP7A and ATP7B) membranes. Following transfer, membranes were blocked in either 5% skim milk (Ctr1, ATP7A, ATP7B, SOD1, and TH), or 1% casein (Atox1), in PBS containing 0.1% Tween® 20 and incubated with appropriate primary antibodies diluted in PBS containing 0.1% Tween® 20 and 1% skim milk (Ctr1, ATP7A, ATP7B, SOD1, and TH) or 1% casein (Atox1) at the following concentrations: Ctr1 (1:200), Atox1 (1:250), ATP7A (1:750), ATP7B (1:1500), SOD1 (1:10,000), and TH (1:5000) overnight at 4 °C. Following incubation with horseradish peroxidase-conjugated mouse anti-goat IgG (1:10,000), goat anti-mouse IgG (1:2,000), donkey anti-sheep/goat IgG (1:2,000), or donkey anti-rabbit IgG (1:5000), protein

signals were obtained using an ECL Western blotting detection system (Bio-Rad) as per the manufacturer's instructions, and developed using the Chemi-Doc XRS (Bio-Rad). Signal intensities were quantified by densitometry using Quantity One® software (Bio-Rad) and normalized to β–actin (1:10,000) levels. TH levels in the SN were quantified by Western blot to provide an indication of dopaminergic cell loss. As expected, TH levels in the PD SN were significantly reduced by 60% ($p=0.013$). Levels of the Cu transporters Ctr1 (subsequently referred to as TH-associated Ctr1 levels), Atox1, ATP7A, and ATP7B were calculated relative to TH levels in the SN.

2.6. Cu transport protein immunohistochemistry

Formalin fixed slide-mounted paraffin-embedded sections (7μm) were antigen retrieved by either incubation with Tris-EDTA buffer (0.01M Tris, 1 mM EDTA, pH 9.0) at 95 °C for 20 mins (Ctr1), or by microwave irradiation in citrate buffer (pH 6.0) for 15 mins (ATP7A and ATP7B). Non-specific peroxidases were blocked with 1% H_2O_2 (Fronine Laboratory Supplies) in 50% ethanol for 30 mins at room temperature. Non-specific antigen sites were blocked with a mixture of 1% bovine serum albumin (BSA; Sigma) and 5% normal horse serum (NHS; Australis) (Ctr1), Animal Free Blocker™ (Vector Laboratories) (ATP7A), or 3% BSA (Sigma) (ATP7B), for 20 mins at room temperature. Primary antibodies for immunohistochemistry were used at the following dilutions: Ctr1 (1:100), ATP7A (1:300), ATP7B (1:1,000). Primary antibodies for Ctr1, ATP7A and ATP7B were detected using biotinylated IgG antibodies (Vector Laboratories) (1:200), followed by Vector Elite Kit tertiary antibody complex (Vector Laboratories) (1:100), and visualized using 3'3'-diaminobenzidine (DAB; Sigma) with a cresyl violet counterstain (Sigma). Images were taken using a Zeiss AxioCam HRc microscope.

2.7. Cu transport protein immunofluorescence

Due to the inherent difficulty of separating positive DAB staining from NM, immunofluorescence staining was performed on midbrain and pons tissue sections to examine the cellular localization of Ctr1, ATP7A, and ATP7B in SN and LC neurons. Formalin fixed free-floating midbrain sections (50 μm; Ctr1; Supplementary Table 3), formalin fixed slide-mounted sections (20 μm; Ctr1; Supplementary Table 1), and formalin fixed slide-mounted paraffin-embedded sections (7 μm; ATP7A, ATP7B; Supplementary Table 3) were antigen retrieved in Tris-EDTA buffer (0.01 M Tris, 1 mM EDTA, pH 9.0) at 95 °C for 25 mins (Ctr1), or citrate buffer (pH 6.0) with microwave irradiation for 15 mins (ATP7A, ATP7B), and permeabilized with 50% ethanol. Non-specific antigen sites were blocked in 10% NHS (Australis; Ctr1), or 0.25% Casein (Sigma; ATP7A, ATP7B) for 1 hour at room temperature and midbrain sections double-stained for the dopaminergic cell marker tyrosine hydroxylase (TH; 1:500) and for Ctr1 (1:25), ATP7A (1:100), or ATP7B (1:400). Primary antibodies were detected using secondary IgG antibodies conjugated to Alexa Fluor® 594 or Alexa Fluor® 488 fluorophores (Invitrogen). Sections were analysed using a Nikon D-Eclipse C1 Si scanning confocal microscope. The cross-reactivity and specificity of the fluorescence reactions were tested by incubating each primary antibody singularly with the secondary antibody solution containing two fluorophores. No cross reactivity was observed.

2.8. SOD1 Activity Assay

SOD activity was determined using SOD determination kit (Sigma, Cat. #19160) according to the manufacturer's instructions. Total SOD activity was measured in supernatants, and SOD2 activity was measured by the addition of 5 mM potassium cyanide (Sigma). SOD1 activity (units/μg protein) was measured as the difference between total SOD, and SOD2, activity. The specific activity of SOD1 was determined by normalizing SOD1 activity (units/μg

protein) to SOD1 protein levels. A single PD case was excluded from analysis due to a medication history of selegiline, demonstrated to increase midbrain SOD1 activity (Takahata et al., 2006).

2.9. Statistical Analyses

Statistical analyses were performed using PASW v18 (SPSS inc.). Univariate analysis of variance followed by Bonferroni's t-test was used to test for differences between groups. Linear regression was used to test for relationships between variables. A p-value of less than 0.05 was accepted as the level of significance.

3. Results

3.1. Decreased Cu precedes regional cell loss in PD

Quantitative analysis of fixed sections by SRXFM (Fig 1A-C) revealed a decrease in NM-associated Cu in the SN from PD and ILBD cases with respect to both age-matched controls (45% decrease in PD, $p<0.0001$ and 48% decrease in ILBD, $p=0.0003$) and AD cases (31% decrease in PD, $p=0.003$ and 34.5% decrease in ILBD, $p=0.007$) (Fig 1A). Our finding of decreased NM-associated Cu levels in the PD SN was confirmed in fresh frozen tissue sections (65%, $p<0.0001$; Fig 2). A representative set of selected SRXFM elemental images from typical NM-containing neurons is shown in Fig 2. SRXFM imaging of single pigmented neurons demonstrated that Cu was colocalized with NM and that there was no change in the spatial distribution of Cu between control and PD cases. Similarly, analysis of NM from LC neurons showed a 55% decrease in Cu content in PD compared with controls ($p=0.001$; Fig 1B) while no differences were seen in the grey matter of the OCx (Fig 1C). This data confirms a specific reduction in Cu within remaining NM-pigmented neurons in PD and

shows that this deficit occurs in cases with ILBD and limited cell loss, suggesting an early deficit that precedes cell death and clinical symptoms.

Complementary to SRXFM, we quantified intraneuronal Cu levels in separate tissue sections using micro-PIXE to assess Cu content in randomly sampled regions (683 μm x 683 μm) of the SN, LC, and OCx (Fig 1D-F). Alignment of the carbon map and optical microscopic view allowed independent quantification of melanized and non-melanized tissue within each region. Elemental concentrations obtained using micro-PIXE were within the range of those obtained using SRXFM. Micro-PIXE analysis of NM-containing neurons confirmed a decrease in Cu-associated NM in PD (54%, p=0.0012) and ILBD (60%, p=0.004) compared with controls (Fig 1D). Importantly, the Cu decrease was also observed in NM from neurons of the LC (Fig 1E) but not in the OCx (Fig 1F).

Quantification of iron (Fe) and zinc (Zn) levels by PIXE revealed a 49% increase in Fe ($p<0.05$) in NM-containing neurons in fresh frozen PD SN compared with fresh frozen control SN, while Zn concentrations were similar between PD and control cases (Supplementary Table 5). These findings were confirmed by SRXFM on an adjacent set of sections (26% increase in Fe, $p< 0.05$, Supplementary Table 6). In contrast, Fe levels were not altered in fixed tissue within multiple individual pigmented neurons, suggesting that chemical fixation masks changes in Fe in PD. No other changes were found for NM-associated elements investigated across the disease groups in either the SN or LC.

3.2. Reduced Ctr1 is an early change in regions of cell loss in PD

TH-associated Ctr1 was significantly reduced in the SN of the PD brain (50% reduction in Ctr1, p=0.017, Fig 3A) and was significantly correlated with TH-associated Cu levels (p=0.036; Fig 3B) and disease duration (p=0.008; Fig 3C). We have previously described in the normal SN (Davies et al., 2013) robust Ctr1 staining localized with NM (Fig 4A). In the

PD SN however, consistent with our Western blot data, NM-associated Ctr1 immunoreactivity was markedly reduced (Fig 4B). Interestingly, this was restricted to SN dopaminergic neurons, as robust Ctr1 NM staining was observed in pigmented neurons in the nearby ventral tegmental area (VTA) and retrorubral field (Fig 4B, inset). NM-associated Ctr1 immunoreactivity in the SN of AD cases was equivalent to that in control cases (Fig 4C), in contrast, a marked reduction in NM-associated Ctr1 immunoreactivity was observed in the majority of SN neurons in cases of ILBD (Fig 4D).

NM-associated Ctr1 staining in the control LC was more variable compared to the consistently robust staining observed in the control SN. However, while neurons strongly expressing Ctr1 were frequently observed in control (Fig 4E) and AD cases (Fig 4G), strong Ctr1 immunoreactivity was rarely observed in the PD (Fig 4F) and ILBD LC (Fig 4H).

We have previously described strong cytoplasmic expression of Ctr1 in neuronal cell bodies in the normal ACC (Davies et al., 2013) (Fig 5A). Interestingly, in contrast to the PD SN and LC, strong cytoplasmic expression of Ctr1 was preserved in the ACC in PD (Fig 5B), consistent with our Western blot data in this brain region (Fig 5C). Immunoreactivity for ATP7A, ATP7B, and Atox1 in SN and ACC did not differ between PD and control cases.

3.3. Increased SOD1 levels relates to reduced Cu levels in regions of cell loss in PD

SOD1 levels and specific activity were not associated with age, PM delay, or tissue pH. Consistent with our previous findings (Davies et al., 2013), in the control brain Cu levels were significantly higher in the SN compared with those in the OCx and ACC ($p=0.001$, $p\leq0.001$, respectively). Confirming the decrease in SN Cu at the neuronal level, total tissue Cu was reduced by 48% in the PD SN compared with control ($p=0.032$). Regional protein levels of SOD1 in the control SN, OCx, and ACC did not vary significantly, and were not correlated with Cu levels; in contrast in the PD SN there was significantly more SOD1 compared with

the OCx and ACC (p=0.002, p=0.007, respectively; Fig 6A and B) and SOD1 levels were correlated with Cu levels (p=0.004; Fig 6C).

3.4. Initial enhancement of SOD1 antioxidant activity in regions affected by late PD pathology

Specific activity of SOD1 did not vary between the regions studied in the control brains (p=1.000; Fig 7), but in contrast, in the PD brains SOD1 specific activity was significantly greater in the ACC compared with the SN (p=0.032; Fig 7), and there was a trend for increased SOD1 specific activity in the parkinsonian ACC compared with the control ACC (p=0.076; Fig 7).

4. Discussion

The current data demonstrate that Cu, and the expression of the Cu transport protein Ctr1, are decreased within the intraneuronal environment of surviving dopaminergic neurons of the SN and LC in ILBD and PD (Fig 1, 2, 3, and 4). As ILBD is suggested to represent preclinical PD (Dickson et al., 2009) and these cases had not taken anti-parkinsonian medications, this suggests these changes occur early in the disease process and are independent of treatment. As Cu and Ctr1 levels were not altered in the degenerating LC in AD, it is unlikely that the reduction in Cu and Ctr1 observed in these regions in PD results simply from neurodegeneration *per se*. Further, as Cu and Ctr1 levels were unchanged in regions that do not degenerate in PD, it appears that this early decrease is specific to regions vulnerable to neuronal cell loss in this disorder.

Our data in the PD brain show an association between decreasing Ctr1 and Cu levels selectively in regions degenerating in PD (Fig 4), with the decrease in Ctr1 in PD enhanced in patients with longer disease durations and greater cell loss (Fig 3). Data from animal models

show that a decrease in Ctr1 leads to significant neuronal dysfunction and death. Deletion of Ctr1 is embryonic lethal and epithelial cell-specific Ctr1 knockout mice display neonatal defects and severe growth and viability abnormalities (Nose et al., 2006). In addition, organisms lacking Ctr1 are deficient in oxidative stress protection (Dancis et al., 1994; De Freitas et al., 2000; Knight et al., 1996). While our data demonstrate a change in Ctr1 in the parkinsonian brain, the regulation of intracellular Cu is complex and other yet to be characterized Cu transport pathways may also be altered in PD. It has recently been shown, for example, that down-regulation of Ctr1 in a murine model of Wilson's disease is linked to the appearance of a redundant mechanism of Cu transport, the 2 kDa Small Copper Carrier, SCC (Gray et al., 2012). A second Ctr protein, structurally related to Ctr1, has also been identified in mammals, designated Copper transporter 2 (Ctr2). This protein has not been identified in human tissue but is thought to play a role in low affinity Cu import (Bertinato et al., 2008) and in intracellular Cu mobilization (Rees and Thiele, 2007).

To determine the functional consequences of reduced intraneuronal Cu, we assessed a key antioxidant cuproprotein in the brain, SOD1, and identified an associated increase in levels of SOD1 protein in the degenerating PD SN (Fig 6A and B). The relationship we observed between Cu and SOD1 levels is consistent with the hypothesis that cellular Cu levels regulate SOD1 expression (Brown et al., 2004; Henchcliffe and Beal, 2008). Despite this increase in SOD1 protein levels, specific activity of SOD1 was unchanged in the PD SN (Fig 7). In contrast, in the ACC, where Cu and Ctr1 levels are normal SOD1 specific activity was increased above that in the SN of the same brains (Fig 7) and there was a trend for SOD1 specific activity to be higher in the parkinsonian, compared with the control ACC (Fig 7). The increased SOD1 specific activity observed in the ACC where Cu levels are normal, but not in the Cu-deficient SN, suggests that a lack of Cu bioavailability may compromise the function of cuproproteins, such as SOD1. In support of this hypothesis, a profound decrease in the

specific activity of another cuproprotein, ceruloplasmin, was recently reported in the SN in PD (Ayton et al., 2012), a finding with likely implications for iron accumulation and subsequent oxidative stress in PD.

Genetic alterations causing dysfunctional Cu transport proteins and reduced brain Cu levels result in severe neurodegeneration, as observed in Menkes disease (Kaler, 2011; Strausak et al., 2001). The current understanding of neuronal death in PD supports a role for α-synuclein and oxidative stress in these degenerative pathways. We have previously shown that the earliest deposition of α-synuclein in the parkinsonian SN occurs on NM (Halliday et al., 2005) and both regional and NM-associated Cu levels are significantly higher in the normal SN and LC compared with other brain regions (Bohic et al., 2008; Davies et al., 2013). High Cu levels promote the formation of oligomeric (toxic) forms of α-synuclein (Binolfi et al., 2010; Rose et al., 2011; Santner and Uversky, 2010; Wright et al., 2009). Our current data suggest that the presence of Cu associated with NM in these most vulnerable neurons may underlie the greater propensity of α-synuclein to abnormally accumulate in pigmented catecholaminergic neurons, compared with non-pigmented brain regions, such as the ACC. Further studies are required to understand the relationships between NM, Cu and α-synuclein and their roles in neuronal death in the parkinsonian brain.

Our data demonstrate decreased cellular copper levels and disrupted copper pathways in vulnerable brain regions in PD, as well regional changes in SOD1 specific activity that reflect the pattern of neurodegeneration in PD. We also show that neuronal SOD1 protein levels are increased in association with a decrease in Ctr1 and Cu levels prior to cell loss in regions most vulnerable to PD-associated neurodegeneration. These changes are enhanced with increasing disease duration. The reduced activity of copper-dependent SOD1 shown here, and that of ceruloplasmin (Ayton et al., 2012), suggests that a reduction in cellular Cu compromises the

ability of these neurons to defend themselves against oxidative stress, consistent with the severity of cell loss observed in these vulnerable regions in the PD brain.

Acknowledgements

Tissues were received from the New South Wales Tissue Resource Centre at the University of Sydney, supported by the National Health and Medical Research Council of Australia, Schizophrenia Research Institute and the National Institute of Alcohol Abuse and Alcoholism (NIH (NIAAA) R24AA012725), and from the Sydney Brain Bank, which is supported by Neuroscience Research Australia, the University of New South Wales and the National Health and Medical Research Council of Australia. The European Synchrotron Radiation Facility is acknowledged for provision of synchrotron radiation beam time (exp MD-304, MD-258). The synchrotron Diamond is acknowledged for provision of beam time (exp. SP7238). The authors are grateful to AIFIRA facility for granted access to nuclear microprobe end-station. This work was supported by research grants from the Partenariats Hubert Curien (PHC)-FAST, the Australian Department of Innovation, Industry, Science and Research International Science Linkage FAST programs, the National Health and Medical Research Council of Australia (project grant to KLD and JFBM), Parkinson's New South Wales (seed grant to KLD), the 36th District of Quota International, AMP, and a donation from Greg Connolly on behalf of the AMP Foundation and Charter Financial Planning. KMD was a recipient of an Australian Postgraduate Award and a Research Excellence Award form the University of New South Wales. DJH was a recipient of a Research Fellowship from the Australian Research Council, and KLD and GMH were recipients of Research Fellowships from the National Health and Medical Research Council of Australia. We thank Tina Geraki for assistance at diamond I18 beamline, Vanessa Krapp for her assistance with immunocytochemical preparations and Francine Carew-Jones for tissue preparation.

Disclosure statement

The authors declare no actual or potential conflicts of interest.

References

Antharam, V., Collingwood, J.F., Bullivant, J.P., Davidson, M.R., Chandra, S., Mikhaylova, A., Finnegan, M.E., Batich, C., Forder, J.R., Dobson, J., 2012. High field magnetic resonance microscopy of the human hippocampus in Alzheimer's disease: quantitative imaging and correlation with iron. NeuroImage 59(2), 1249-1260.

Ayton, S., Lei, P., Duce, J.A., Wong, B.X., Sedjahtera, A., Adlard, P.A., Bush, A.I., Finkelstein, D.I., 2012. Ceruloplasmin dysfunction and therapeutic potential for parkinson disease. Ann Neurol 73(4), 554-559.

Battaglia, G., Fornai, F., Busceti, C.L., Aloisi, G., Cerrito, F., De Blasi, A., Melchiorri, D., Nicoletti, F., 2002. Selective blockade of mGlu5 metabotropic glutamate receptors is protective against methamphetamine neurotoxicity. J Neurosci 22(6), 2135-2141.

Bertinato, J., Swist, E., Plouffe, L.J., Brooks, S.P., L'Abbe M, R., 2008. Ctr2 is partially localized to the plasma membrane and stimulates copper uptake in COS-7 cells. Biochem J 409(3), 731-740.

Binolfi, A., Rodriguez, E.E., Valensin, D., D'Amelio, N., Ippoliti, E., Obal, G., Duran, R., Magistrato, A., Pritsch, O., Zweckstetter, M., Valensin, G., Carloni, P., Quintanar, L., Griesinger, C., Fernandez, C.O., 2010. Bioinorganic chemistry of Parkinson's disease: structural determinants for the copper-mediated amyloid formation of alpha-synuclein. Inorg Chem 49(22), 10668-10679.

Bohic, S., Murphy, K., Paulus, W., Cloetens, P., Salome, M., Susini, J., Double, K., 2008. Intracellular chemical imaging of the developmental phases of human neuromelanin using synchrotron X-ray microspectroscopy. Anal Chem 80(24), 9557-9566.

Botella, J.A., Bayersdorfer, F., Schneuwly, S., 2008. Superoxide dismutase overexpression protects dopaminergic neurons in a Drosophila model of Parkinson's disease. Neurobiol Dis 30(1), 65-73.

Braak, H., Del Tredici, K., Rub, U., de Vos, R.A., Jansen Steur, E.N., Braak, E., 2003. Staging of brain pathology related to sporadic Parkinson's disease. Neurobiology of aging 24(2), 197-211.

Brown, N.M., Torres, A.S., Doan, P.E., O'Halloran, T.V., 2004. Oxygen and the copper chaperone CCS regulate posttranslational activation of Cu,Zn superoxide dismutase. Proc Natl Acad Sci U S A 101(15), 5518-5523.

Carmona, A., Deves, G., Ortega, R., 2008. Quantitative micro-analysis of metal ions in subcellular compartments of cultured dopaminergic cells by combination of three ion beam techniques. Analytical and bioanalytical chemistry 390(6), 1585-1594.

Cater, M.A., La Fontaine, S., Mercer, J.F., 2007. Copper binding to the N-terminal metal-binding sites or the CPC motif is not essential for copper-induced trafficking of the human Wilson protein (ATP7B). Biochem J 401(1), 143-153.

Dancis, A., Haile, D., Yuan, D.S., Klausner, R.D., 1994. The Saccharomyces cerevisiae copper transport protein (Ctr1p). Biochemical characterization, regulation by copper, and physiologic role in copper uptake. J Biol Chem 269(41), 25660-25667.

Davies, K.M., Hare, D.J., Cottam, V., Chen, N., Hilgers, L., Halliday, G., Mercer, J.F., Double, K.L., 2013. Localization of copper and copper transporters in the human brain. Metallomics : integrated biometal science 5(1), 43-51.

de Bie, P., Muller, P., Wijmenga, C., Klomp, L.W., 2007. Molecular pathogenesis of Wilson and Menkes disease: correlation of mutations with molecular defects and disease phenotypes. Journal of medical genetics 44(11), 673-688.

De Freitas, J.M., Liba, A., Meneghini, R., Valentine, J.S., Gralla, E.B., 2000. Yeast lacking Cu-Zn superoxide dismutase show altered iron homeostasis. Role of oxidative stress in iron metabolism. J Biol Chem 275(16), 11645-11649.

Dexter, D.T., Wells, F.R., Lees, A.J., Agid, F., Agid, Y., Jenner, P., Marsden, C.D., 1989. Increased nigral iron content and alterations in other metal ions occurring in brain in Parkinson's disease. J Neurochem 52(6), 1830-1836.

Dickson, D.W., Braak, H., Duda, J.E., Duyckaerts, C., Gasser, T., Halliday, G.M., Hardy, J., Leverenz, J.B., Del Tredici, K., Wszolek, Z.K., Litvan, I., 2009. Neuropathological assessment of Parkinson's disease: refining the diagnostic criteria. Lancet neurology 8(12), 1150-1157.

Gray, L.W., Peng, F., Molloy, S.A., Pendyala, V.S., Muchenditsi, A., Muzik, O., Lee, J., Kaplan, J.H., Lutsenko, S., 2012. Urinary copper elevation in a mouse model of Wilson's disease is a regulated process to specifically decrease the hepatic copper load. PloS one 7(6), e38327.

Halliday, G.M., Ophof, A., Broe, M., Jensen, P.H., Kettle, E., Fedorow, H., Cartwright, M.I., Griffiths, F.M., Shepherd, C.E., Double, K.L., 2005. Alpha-synuclein redistributes to neuromelanin lipid in the substantia nigra early in Parkinson's disease. Brain : a journal of neurology 128(Pt 11), 2654-2664.

Harding, A.J., Stimson, E., Henderson, J.M., Halliday, G.M., 2002. Clinical correlates of selective pathology in the amygdala of patients with Parkinson's disease. Brain : a journal of neurology 125(Pt 11), 2431-2445.

Henchcliffe, C., Beal, M.F., 2008. Mitochondrial biology and oxidative stress in Parkinson disease pathogenesis. Nature clinical practice Neurology 4(11), 600-609.

Hirsch, E., Graybiel, A.M., Agid, Y.A., 1988. Melanized dopaminergic neurons are differentially susceptible to degeneration in Parkinson's disease. Nature 334(6180), 345-348.

Kaler, S.G., 2011. ATP7A-related copper transport diseases-emerging concepts and future trends. Nat Rev Neurol 7(1), 15-29.

Ke, B.X., Llanos, R.M., Wright, M., Deal, Y., Mercer, J.F., 2006. Alteration of copper physiology in mice overexpressing the human Menkes protein ATP7A. Am J Physiol Regul Integr Comp Physiol 290(5), R1460-1467.

Knight, S.A., Labbe, S., Kwon, L.F., Kosman, D.J., Thiele, D.J., 1996. A widespread transposable element masks expression of a yeast copper transport gene. Genes & development 10(15), 1917-1929.

Larner, F., Sampson, B., Rehkamper, M., Weiss, D.J., Dainty, J.R., O'Riordan, S., Panetta, T., Bain, P.G., 2013. High precision isotope measurements reveal poor control of copper metabolism in Parkinsonism. Metallomics : integrated biometal science 5(2), 125-132.

Loeffler, D.A., LeWitt, P.A., Juneau, P.L., Sima, A.A., Nguyen, H.U., DeMaggio, A.J., Brickman, C.M., Brewer, G.J., Dick, R.D., Troyer, M.D., Kanaley, L., 1996. Increased regional brain concentrations of ceruloplasmin in neurodegenerative disorders. Brain Res 738(2), 265-274.

Lombardo, M.F., Ciriolo, M.R., Rotilio, G., Rossi, L., 2003. Prolonged copper depletion induces expression of antioxidants and triggers apoptosis in SH-SY5Y neuroblastoma cells. Cell Mol Life Sci 60(8), 1733-1743.

McCord, J.M., Fridovich, I., 1969. Superoxide dismutase. An enzymic function for erythrocuprein (hemocuprein). J Biol Chem 244(22), 6049-6055.

Meloni, G., Vasak, M., 2011. Redox activity of alpha-synuclein-Cu is silenced by Zn(7)-metallothionein-3. Free Radic Biol Med 50(11), 1471-1479.

Montine, T.J., Phelps, C.H., Beach, T.G., Bigio, E.H., Cairns, N.J., Dickson, D.W., Duyckaerts, C., Frosch, M.P., Masliah, E., Mirra, S.S., Nelson, P.T., Schneider, J.A., Thal, D.R., Trojanowski, J.Q., Vinters, H.V., Hyman, B.T., 2012. National Institute on Aging-Alzheimer's Association guidelines for the neuropathologic assessment of Alzheimer's disease: a practical approach. Acta neuropathologica 123(1), 1-11.

Nose, Y., Kim, B.E., Thiele, D.J., 2006. Ctr1 drives intestinal copper absorption and is essential for growth, iron metabolism, and neonatal cardiac function. Cell Metab 4(3), 235-244.

Popescu, B.F., Robinson, C.A., Rajput, A., Rajput, A.H., Harder, S.L., Nichol, H., 2009. Iron, copper, and zinc distribution of the cerebellum. Cerebellum 8(2), 74-79.

Prohaska, J.R., 1983. Comparison of copper metabolism between brindled mice and dietary copper-deficient mice using 67Cu. J Nutr 113(6), 1212-1220.

Rees, E.M., Thiele, D.J., 2007. Identification of a vacuole-associated metalloreductase and its role in Ctr2-mediated intracellular copper mobilization. J Biol Chem 282(30), 21629-21638.

Rose, F., Hodak, M., Bernholc, J., 2011. Mechanism of copper(II)-induced misfolding of Parkinson's disease protein. Scientific reports 1, 11.

Santner, A., Uversky, V.N., 2010. Metalloproteomics and metal toxicology of alpha-synuclein. Metallomics : integrated biometal science 2(6), 378-392.

Schaefer, M., Gitlin, J.D., 1999. Genetic disorders of membrane transport. IV. Wilson's disease and Menkes disease. Am J Physiol 276(2 Pt 1), G311-314.

Strausak, D., Mercer, J.F., Dieter, H.H., Stremmel, W., Multhaup, G., 2001. Copper in disorders with neurological symptoms: Alzheimer's, Menkes, and Wilson diseases. Brain Res Bull 55(2), 175-185.

Takahata, K., Shimazu, S., Katsuki, H., Yoneda, F., Akaike, A., 2006. Effects of selegiline on antioxidant systems in the nigrostriatum in rat. J Neural Transm 113(2), 151-158.

Torsdottir, G., Sveinbjornsdottir, S., Kristinsson, J., Snaedal, J., Johannesson, T., 2006. Ceruloplasmin and superoxide dismutase (SOD1) in Parkinson's disease: a follow-up study. J Neurol Sci 241(1-2), 53-58.

Tripanichkul, W., Sripanichkulchai, K., Duce, J.A., Finkelstein, D.I., 2007. 17Beta-estradiol reduces nitrotyrosine immunoreactivity and increases SOD1 and SOD2 immunoreactivity in nigral neurons in male mice following MPTP insult. Brain Res 1164, 24-31.

Uitti, R.J., Rajput, A.H., Rozdilsky, B., Bickis, M., Wollin, T., Yuen, W.K., 1989. Regional metal concentrations in Parkinson's disease, other chronic neurological diseases, and control brains. Can J Neurol Sci 16(3), 310-314.

Wang, X., Moualla, D., Wright, J.A., Brown, D.R., 2010. Copper binding regulates intracellular alpha-synuclein localisation, aggregation and toxicity. J Neurochem 113(3), 704-714.

Wright, J.A., Wang, X., Brown, D.R., 2009. Unique copper-induced oligomers mediate alpha-synuclein toxicity. FASEB J 23(8), 2384-2393.

Figure legends

Figure 1. Intraneuronal copper (Cu) levels measured in fixed brain tissue by Synchrotron X-ray fluorescence microscopy (A-C) and particle induced X-ray emission (PIXE) microprobes (D-F). Intraneuronal Cu levels were significantly reduced in the Parkinson's disease (Parkinson) and Incidental Lewy Body disease (ILBD) substantia nigra (SN), compared to control (Normal), but remained unchanged in the Alzheimer's disease (AD) SN (A, D). Intraneuronal Cu levels were significantly reduced in the Parkinson's locus coeruleus (LC), compared to control (B, E), while Cu levels remained unchanged in the Parkinson's and AD occipital cortex (OCx) (C, F). Bars are mean ± SEM. The numbers of samples analyzed by PIXE and/or Synchrotron X-ray fluorescence microscopy are reported in Supplementary Table 5 and 6, respectively. Significant differences were determined by multivariate analysis of variance (ANOVA), $p<0.05$.

Figure 2. Representative map for copper (Cu) obtained from single intact neuromelanin-containing neurons in the substantia nigra (SN) of a Parkinson's disease (Parkinson, n=5) and control (Normal, n=5) case, by Synchrotron X-ray fluorescence microscopy (A, B). The X-ray fluorescence signal intensity is shown as a color scale. Intraneuronal Cu levels, measured in fresh frozen tissue sections, were significantly reduced in the Parkinson's disease SN compared to normal controls (C). Bars in (C) are mean ± SEM. Significant differences between normal and Parkinson's brains* were determined by two-tailed t-test, $p<0.05$.

Figure 3. Tyrosine hydroxylase (TH)-associated Copper transporter 1 (Ctr1) levels in the substantia nigra in Parkinson's disease (Parkinson) (n=7) were significantly reduced compared with controls (Normal) (n=6) (A) and were positively correlated with TH-associated copper (Cu) levels (B) and disease duration (C). Ctr1 and TH levels were

quantified by densitometry performed on Western blots and normalized to β-actin levels (used as a loading control). Cu levels were determined by inductively coupled plasma-mass spectrometry and calculated relative to TH levels. Bars in (A) are mean ± SEM. Significant differences between normal and Parkinson's brains* were determined by Univariate analysis of variance followed by Bonferroni-corrected posthoc t-tests.

Figure 4. Representative photomicrographs of Copper transporter 1 (Ctr1) in the control (Normal) (A, E), Parkinson's disease (B, F), Alzheimer's disease (AD) (C, G), and Incidental Lewy Body disease (ILBD) (D, H) substantia nigra pars compacta dopaminergic neurons (A-D) and locus coeruleus noradrenergic neurons (E-H). Midbrain and pons sections were dual stained for dopaminergic marker, tyrosine hydroxylase (TH; green), and Ctr1 (red). Insets: no Ctr1 primary control (A) and Parkinson's disease (B) neurons from the ventral tegmental area positively stained for Ctr1.

Figure 5. The cellular localization (A-B) and levels (C) of the copper transport protein Copper transporter 1 (Ctr1) in the anterior cingulate cortex (ACC) of the normal control (n=7) (A) and Parkinson's disease (n=6) (B) brain. Cellular localization was investigated on 7μm paraffin embedded sections probed for Ctr1 using peroxidase immunohistochemistry (brown) with cresyl violet counterstain. Regions of positive staining are dark brown. Scale bar in B applies to A and B. Ctr1 levels (C) were quantified by densitometry performed on Western blots and normalized to β-actin levels (used as a loading control). Values are mean ± SEM. Differences between normal and Parkinson's brains were determined by Univariate analysis of variance followed by Bonferroni-corrected posthoc t-tests.

Figure 6. Superoxide dismutase 1 (SOD1) levels in the substantia nigra (SN), anterior cingulate cortex (ACC) and occipital cortex (OCx) of the normal and Parkinson's disease brain (A). SOD1 levels were quantified by densitometry performed on Western blots and normalized to β-actin levels (used as a loading control) (B). Values are mean ± SEM. Significant differences between regions in normal and Parkinson's brains, determined by Univariate analysis of variance followed by Bonferroni-corrected posthoc t-tests, are indicated*. Normal SN, n=8; ACC, n=8; and OCx, n=8. PD SN, n=7; ACC, n=7; and OCx, n=7. SOD1 levels were significantly associated with copper (Cu) levels in the Parkinson's disease brain, but not in normal controls (C). Cu levels were determined by inductively coupled plasma-mass spectrometry.

Figure 7. Superoxide dismutase 1 (SOD1) specific activity in the substantia nigra (SN), anterior cingulate cortex (ACC), and occipital cortex (OCx) of the normal and Parkinson's disease brain. SOD1 specific activity was not significantly different between brain regions in control cases (Normal), but was significantly disrupted in the Parkinson's disease brain in regions affected by α-synuclein pathology (SN and ACC), in a manner that reflected cellular vulnerability (p=0.032*). There was a strong trend (p=0.076) for SOD1 specific activity in the PD ACC to be greater than that in the control ACC. Values are mean ± SEM. Differences between brain regions within diagnostic groups and between normal and Parkinson's brains were determined by Univariate analysis of variance followed by Bonferroni-corrected posthoc t-tests. Normal SN, n=8; ACC, n=8; and OCx, n=8. PD SN, n=6; ACC, n=7; and OCx, n=6. SOD1 specific activity was determined by normalizing SOD1 activity (units/μg protein) to SOD1 protein levels.

Figures

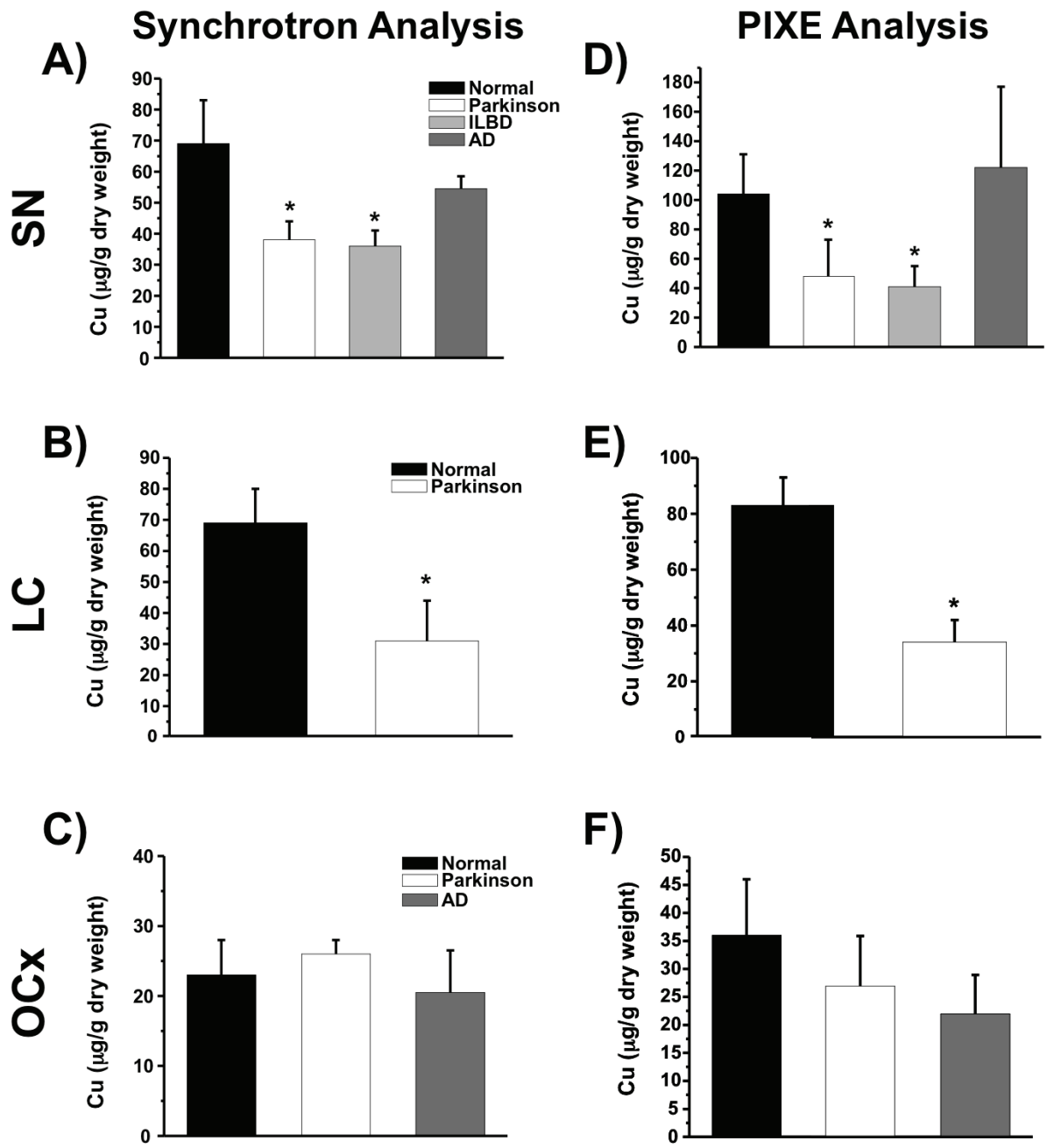

Figure 1

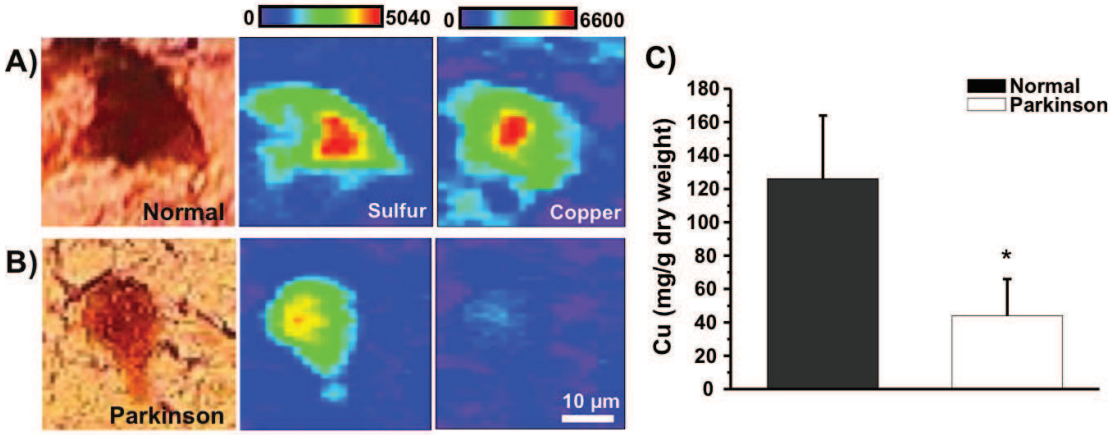

Figure 2

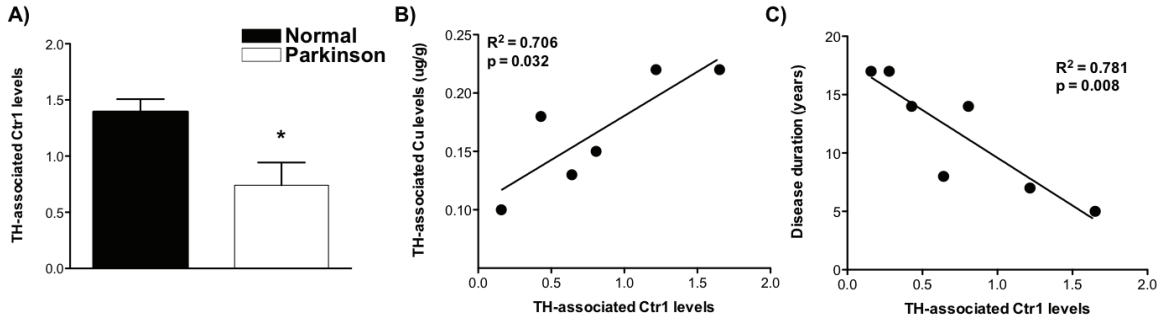

Figure 3

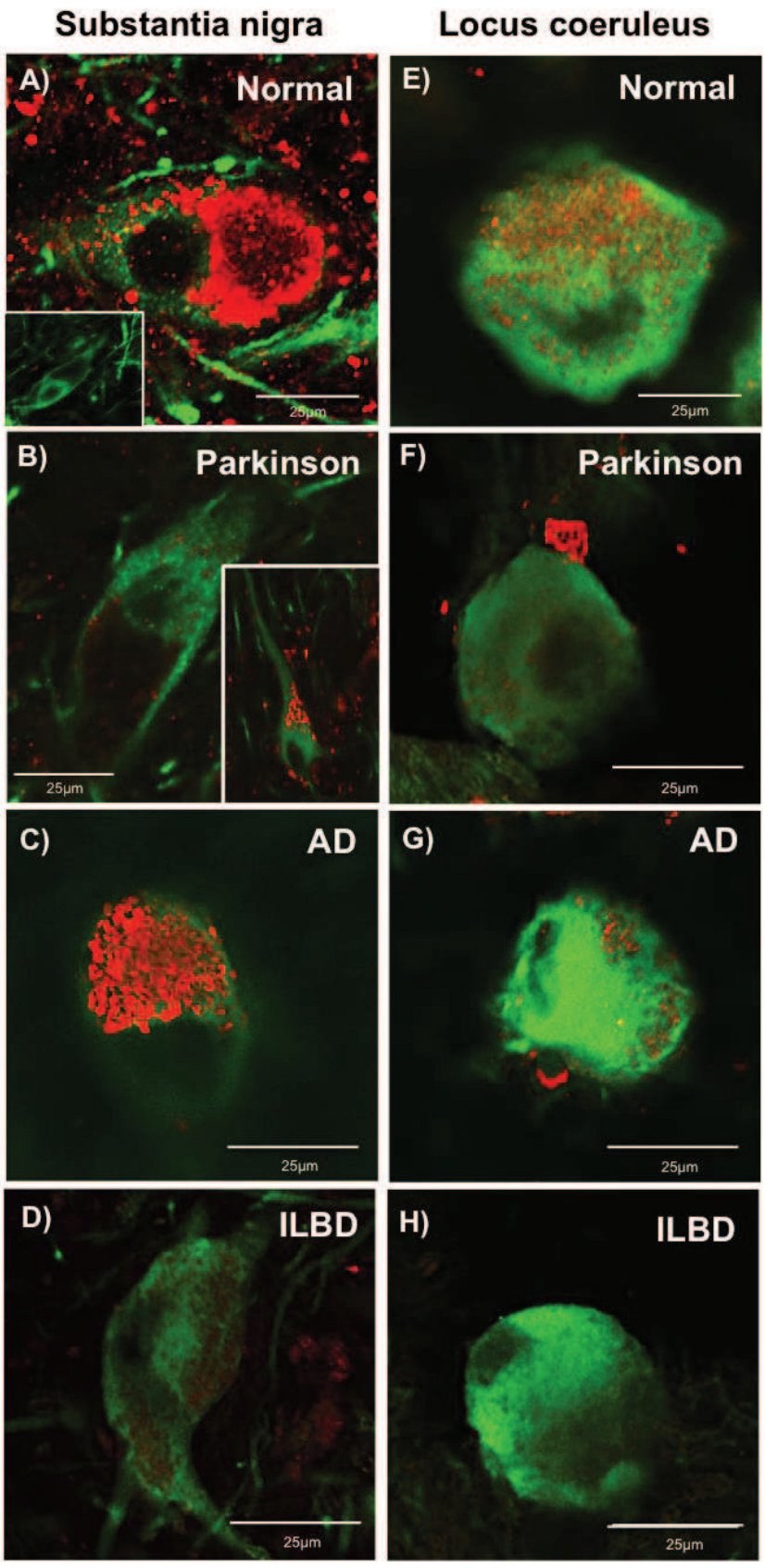

Figure 4

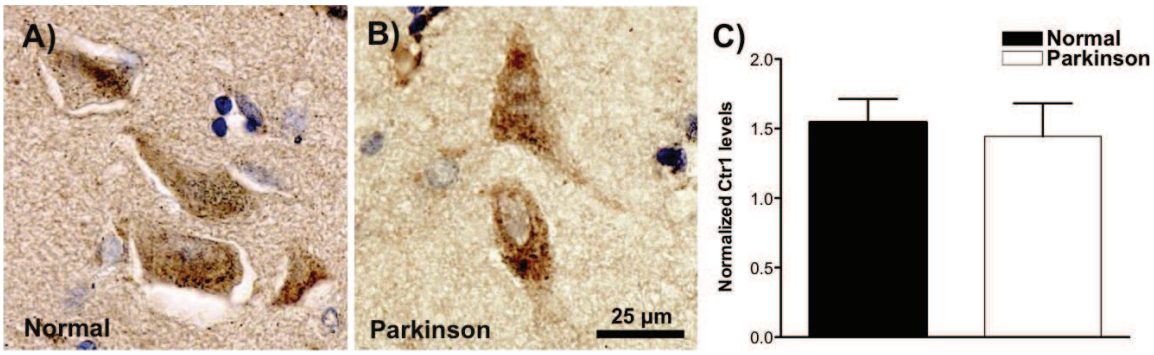

Figure 5

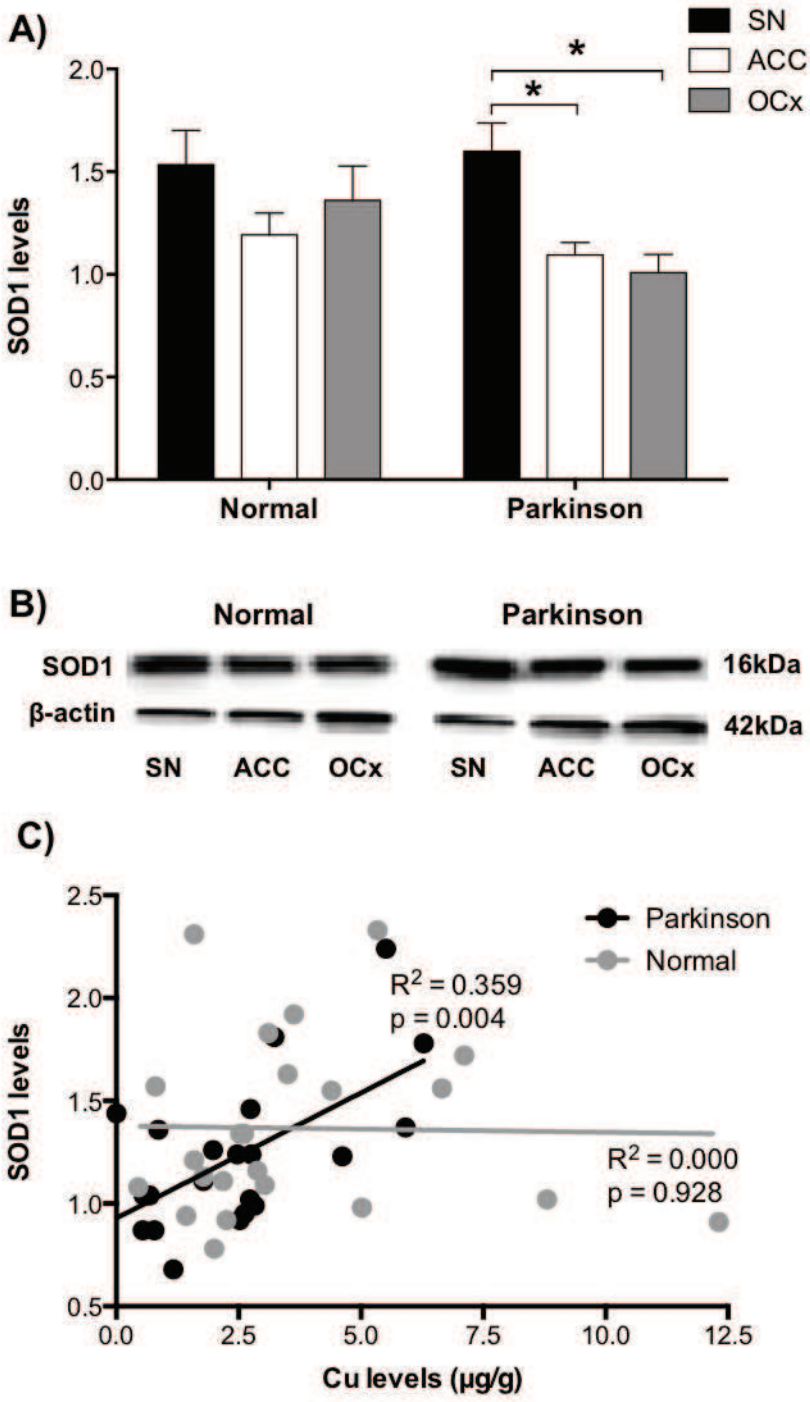

Figure 6

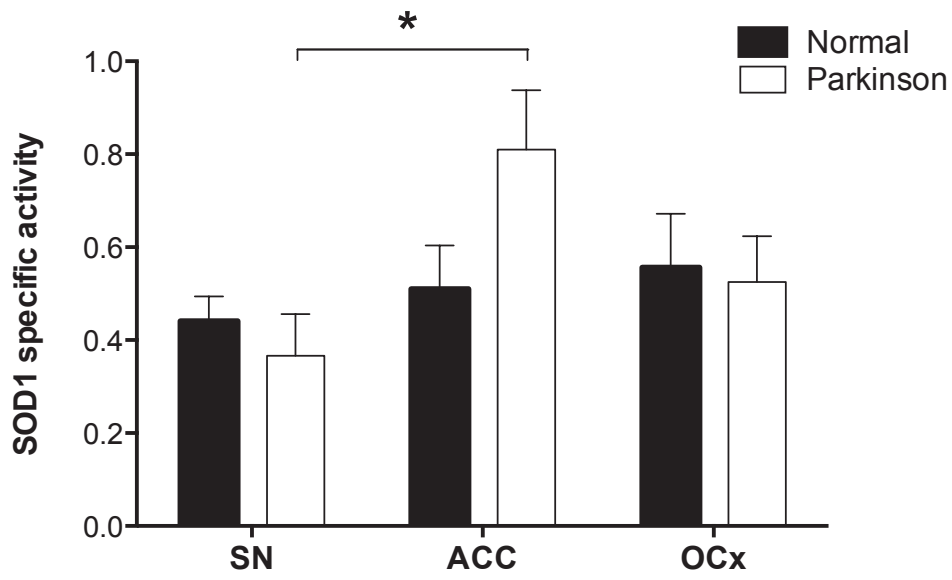

Figure 7

Supplementary Information

Supplementary Table 1

Subject Demographics	Control subjects (N=10)	PD Patients (N=10)	ILBD Patients (N=3)	AD Patients (N=6)
Sex f/m	7/3	7/3	0/3	4/2
Age (years) (range)	82.4±10.2 (69-98)	77.6±8.7 (69-92)	79±10.1 (68-88)	78.3±6.8 (74-88)
pmd (hrs)	25.6±13.5	21.9±9.1	55.3±27.2	17.8±15.8
Tissue pH (range)	7.2 – 7.4	7.2 – 7.4	7.2 – 7.4	7.2 – 7.4
Time in fixative (years)	2.4±1.2	2.8±1.5	2.8±0.3	3.0±0.9
DD (years)	–	12.7±4.3	–	9.5±4.6
H/Y stage	–	5 patients stage 5 – DD 5-16 y 3 patients stage 4 – DD 10-20 y 1 patient stage 3 – DD 13 y 1 patient stage 2 – DD 6 y	–	–
Duration of L-dopa treatment (years)	–	11.5±4	–	–

Tissue characteristics and clinical data for formalin fixed samples studied using synchrotron X-ray fluorescence and PIXE microprobes to measure cellular copper levels, and for immunofluorescence studies of cuproprotein localization. Regions investigated include the substantia nigra, locus coeruleus, and occipital cortex. Values are presented as mean ± SD and/or range. PD = Parkinson's disease, ILBD = Incidental Lewy Body Disease, AD = Alzheimer's disease, f = female, m = male, pmd = Post-mortem delay, DD = Disease duration, H/Y stage = Hoehn and Yahr stage.

Supplementary Table 2

Subject Demographics	Control subjects (N=5)	PD Patients (N=5)
Sex f/m	1/4	1/4
Age (years) (range)	82.4±6.0 (73-88)	80.6±6.3 (73-90)
pmd (hrs)	21.7±16.1	21.9±9.1
Tissue pH (range)	6.28 –6.75	6.25 –6.69
Storage time in freezer (years)	2.9±1.1	3.0±1.2
DD (years)	–	16.6±3.9
H/Y stage	–	3 patients stage 5 – DD 13-15 y 2 patients stage 4 – DD 17,24 y

Tissue characteristics and clinical data for fresh frozen samples studied using synchrotron X-ray fluorescence and PIXE microprobes to determine cellular copper levels in the substantia nigra. Values are presented as mean ± SD and/or range. PD = Parkinson's disease, f = female, m = male, pmd = Post-mortem delay, DD = Disease duration, H/Y stage = Hoehn and Yahr stage.

Supplementary Table 3

	Fresh frozen		Fixed	
Subject Demographics	**Control subjects (N=8)**	**PD Patients (N=7)**	**Control subjects (N=3)**	**PD Patients (N=3)**
Sex f/m	2/6	2/5	1/2	1/2
Age (years) (range)	69±28 (41-103)	80±7 (69-90)	93±10 (84-103)	78±4 (74-82)
pmd (hrs)	23±6.9	12±7.6	24±20.3	32±13.7
Tissue pH	5.9 – 7.0	5.9 – 6.8	6.1 – 6.7	5.9 – 7.0
DD (years)	–	11.7±4.3	–	7.3±0.6
H/Y stage	–	1 patient stage 6 – DD 8 yrs 6 patients stage 5 – DD 5-17 yrs	–	3 patients stage 6 – DD 7-8 yrs

Case details for tissues investigated for cuproprotein levels (fresh frozen) and cellular localization (fixed), and SOD1 activity (fresh frozen). Regions investigated include the substantia nigra, anterior cingulate, and occipital cortices. Tissue characteristics and clinical data presented as mean +/- SD and (range). PD = Parkinson's disease, ILBD = Incidental Lewy Body Disease, AD = Alzheimer's disease, f = female, m = male, pmd = Post-mortem delay, DD = Disease duration, H/Y stage = Hoehn and Yahr stage.

Supplementary Table 4

Antigen	Immunogen	Source
Ctr1	Peptide mapping within amino acids 100-150 of CTR1 of human origin.	Santa Cruz Biotechnology, Inc. (CA, USA); CTR1 (G-15); goat polyclonal.
Atox1	ATOX1 (NP_004036, 1 a.a. – 68a.a.) partial recombinant protein with GST tag.	Abnova (Taiwan); ATOX1, clone 2E6; mouse monoclonal.
ATP7A	First 590 N-terminal amino acids of the human MNK protein.	In-house original antibody; R17; sheep polyclonal (Ke et al., 2006).
ATP7B	36-kDa fusion protein with a His6 tag at the N-terminus of the protein comprising amino acids 1-199 (N-terminal), 1309-1315 and 1376-1465 (C-terminal) of the human ATP7B protein.	In-house original antibody; NC36; sheep polyclonal (Cater et al., 2007).
SOD1	Highly purified, human erythrocyte SOD Cu/Zn.	Chemicon (Millipore) (Billerica, MA, USA); Anti-Superoxide Dismutase (Cu/Zn Enzyme); sheep polyclonal.
β-actin	Amino acids 50-70 of purified chicken gizzard actin.	Millipore (Billerica, MA, USA); Anti-Actin, clone C4; mouse monoclonal
TH (IF)	Amino acids 1-196 of TH of human origin.	Santa Cruz Biotechnology, Inc. (CA, USA); TH (H-196); rabbit polyclonal.
TH (WB)	Denatured tyrosine hydroxylase from rat pheochromocytoma.	Chemicon (Millipore) (Billerica, MA, USA); Anti-Tyrosine Hydroxylase Antibody; rabbit polyclonal.

Primary antibodies.

Supplementary Table 5

Brain regions		Fe	Cu	Zn
Occipital cortex	**Normal** (N=4)	**225** *(24)*	**36** *(10)*	**83** *(32)*
	PD (N=4)	**188** *(36)*	**27** *(9)*	**78** *(24)*
	AD (N=3)	**261** *(48)*	**22** *(7)*	**79** *(32)*
SN tissue	**Normal** (N=8)	**699** *(388)*	**81** *(23)*	**147** *(60)*
	PD (N=7)	**500** *(266)*	**36** *(9)*	**86** *(37)*
	ILBD (N=2)	**708** *(136)*	***42*** *(27)*	***177*** *(76)*
	AD (N=6)	**814** *(197)*	***88*** *(16)*	***193*** *(63)*
SN Neuromelanin	**Normal** (N=8)	**1799** *(771)*	**104** *(27)*	**196** *(65)*
	PD (N=7)	**924** *(229)*	**48** *(25)*	**102** *(38)*
	ILBD (N=2)	**1306** *(277)*	**41** *(14)*	**201** *(88)*
	AD (N=6)	**1668** *(574)*	**122** *(55)*	**321** *(29)*
	Normal frozen (N=5)	**1105** *(347)*	**126** *(38)*	**153** *(24)*
	PD frozen (N=5)	**1646** *(353)*	**44** *(23)*	**128** *(33)*
LC Neuromelanin	**Normal** (N=4)	**588** *(114)*	**83** *(10)*	**107** *(21)*
	PD (N=4)	**759** *(258)*	**34** *(8)*	**111** *(24)*

Iron (Fe), copper (Cu) and zinc (Zn) concentrations, determined by Particle-Induced X-Ray Emission (PIXE), in the occipital cortex, substantia nigra pars compacta (SN), and within neuromelanin (NM) of neurons from the substantia nigra pars compacta (SN) and locus

coeruleus (LC) of Parkinson's disease (PD), Incidental Lewy Body Disease (ILBD) and Alzheimer's disease (AD) patients, compared with normal controls. All tissues were chemically fixed, unless otherwise stated, in which case fresh frozen sections were analysed. Data reported as mean elemental concentrations, expressed as μg/g dry weight, with standard deviations reported in parentheses.

Supplementary Table 6:

Brain regions		Fe	Cu	Zn
Occipital cortex	**Normal** (N=4)	**222.5** *(13)*	**23** *(5)*	**94** *(7)*
	PD (N=4)	**209** *(7.5)*	**26** *(2)*	**84** *(17)*
	AD (N=3)	**227** *(14)*	**20.5** *(6)*	**92** *(9)*
SN Neuromelanin	**Normal** (N=10)	**2135** *(805)*	**69** *(14)*	**206** *(55)*
	PD (N=10)	**1910** *(709)*	**38** *(6)*	**196** *(63)*
	ILBD (N=3)	**796** *(146)*	**36** *(5)*	**112** *(26)*
	AD (N=5)	**1685** *(290)*	**55** *(4)*	**238** *(90)*
	Normal frozen (N=5)	**1267** *(229)*	**81** *(10)*	**154** *(38)*
	PD frozen (N=5)	**1594** *(187)*	**29** *(6)*	**134** *(25)*
LC Neuromelanin	**Normal** (N=5)	**826** *(225)*	**69** *(11)*	**153** *(43)*
	PD (N=5)	**1086** *(397)*	**31** *(13)*	**186** *(43)*

Iron (Fe), copper (Cu) and zinc (Zn) concentrations, determined by synchrotron X-ray fluorescence microscopy, in the occipital cortex and within neuromelanin (NM) of neurons from the substantia nigra pars compacta (SN) and locus coeruleus (LC) of Parkinson's disease (PD), Incidental Lewy Body Disease (ILBD) and Alzheimer's disease (AD) patients, compared with normal controls. All tissues were chemically fixed, unless otherwise stated, in which case fresh frozen sections were analysed. Data reported as mean elemental concentrations, expressed as μg/g dry weight, with standard deviations reported in parentheses.

Supplementary Figure 1: Representative map for sulfur (S), iron (Fe), copper (Cu), zinc (Zn) and selenium (Se) obtained from single intact neuromelanin-containing neurons in the substantia nigra (SN) of healthy normal (a and b), Parkinson's disease (c and d), Incidental Lewy body disease (e), and Alzheimer's disease (f) cases, by Synchrotron X-ray fluorescence microscopy. a) and d) are from human fresh frozen SN while all other images are from chemically fixed human SN. The X-ray fluorescence signal intensity is shown as a color scale and allows for the comparison of each elemental map for the different cases. Scale bars, 10 µm.

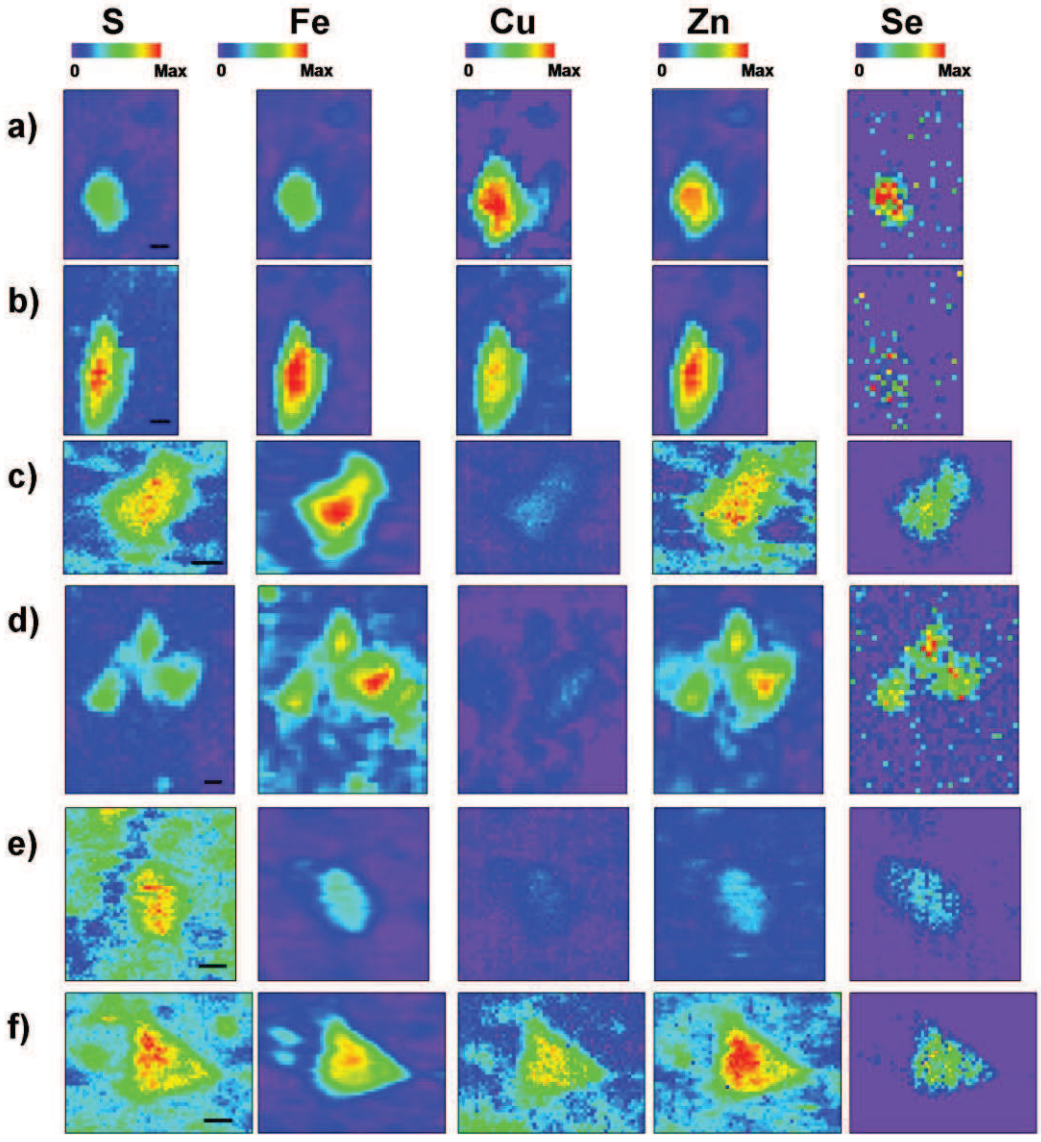

Supplementary Figure 2: Representative map for sulfur (S), iron (Fe), copper (Cu), zinc (Zn) and selenium (Se) obtained from single intact neuromelanin-containing neurons in the locus coeruleus (LC) of a healthy normal (a) and Parkinson's disease (PD) (b) case, by Synchrotron X-ray fluorescence microscopy. All tissues are from chemically fixed human LC. The X-ray fluorescence signal intensity is shown as a color scale and allows for the comparison of each elemental map for healthy normal and PD cases. Scale bars, 10 µm.